

# Flexible order parameters for quantifying the rate-dependent energy release mechanism of Au nanowires

Christopher R. Iacovella<sup>1</sup>, William R. French<sup>1</sup>, Peter T. Cummings<sup>1,2</sup>

<sup>1</sup>Department of Chemical and Biomolecular Engineering, Vanderbilt University, Nashville, TN 37235-1604

<sup>2</sup> Center for Nanophase Materials Sciences, Oak Ridge National Laboratory, Oak Ridge, TN 37831-6494

E-mail: c.iacovella@vanderbilt.edu

**Abstract.** In this work, we develop order parameters to detect the structural changes that occur as Au nanowires are mechanically deformed. These order parameters are developed in the context of shape matching, allowing us to create highly specialized order parameters within a single, general framework. We use these order parameters to quantify the rate and temperature-dependent behavior of mechanically deformed nanowires. The results of our structural analysis quantify and confirm the recently discovered rate-dependent energy release mechanism that dictates the relaxation modes of the nanowires.

## 1. Introduction

Nanowires undergoing mechanical deformation are known to demonstrate a variety of unique behaviors related to the structural relaxation of the wire, such as quantized conductance [1, 2] and the formation of monatomic chains [3, 4]. Simulation and theory have thus far played a vital role in understanding the behavior of these nanowire systems [5–8], due in large part to their ability to resolve the full temporal and spatial coordinates of the atoms. Access to this information has facilitated the direct observation of behavior that is inaccessible to experiment, such as correlating the transport [9–11] and bandgap [12] properties directly with the local structure of atoms. Fully resolved coordinates have additionally enabled researchers to directly observe modes by which nanowires relax their structure in response to applied tensile forces. Previous simulation studies from our group [6] revealed a rate-dependent energy release mechanism for Au nanowires that dictates which structural relaxation modes are likely to occur as the nanowires elongate. For example, high energy structural motifs, such as long monatomic chains, are more likely to form in systems at low temperature or in systems elongated at high rates; conversely, low-energy motifs, such as crystal dislocations and reorientations, are more likely to occur at high temperature or for systems pulled at low elongation rates.

To date, most simulation studies of nanowire elongation, including those from our group, have relied on either visual inspection or indirect measures of structure, such as potential energy or tensile force, to identify key structural changes. In this work, we illustrate the use of specialized structural order parameters to directly quantify the key changes in mechanically deformed nanowires. Our approach builds from the computer science field of “shape matching” [13],

as this allows us to develop specialized, ad hoc order parameters within a single, general framework [14, 15]. We introduce two example structural metrics to calculate (i) the local structural correlation of an atom as a function of elongation and (ii) the onset of neck formation. We apply these metrics to trajectories resulting from molecular dynamics simulations of Au nanowires, performed using the many-body tight-binding second-moment approximation (TB-SMA) potential. We demonstrate the utility of these metrics by exploring trends as a function of rate of elongation for different temperatures, in order to further quantify the rate-dependent energy release mechanism proposed in reference [6].

## 2. Methods

### 2.1. Simulation method and model

As in our previous work [5, 6], the continuous stretching of a face-centered cubic (FCC) gold nanowire is approximated by using a stretch-and-relax technique in which two layers of grip atoms (colored red in Fig. 1) are periodically displaced a small amount ( $0.1 \text{ \AA}$ ) in the  $[100]$  direction. Two layers of grip atoms also reside on the opposite end of the wire (colored green in Fig. 1). All grip atoms are held fixed during the simulation, while atoms within the core of the wire (colored yellow in Fig. 1) are dynamic. The elongation rate is controlled by varying the frequency at which the grip atoms are displaced.

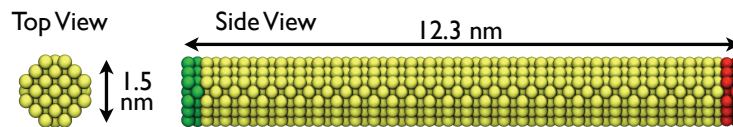


**Figure 1.** Schematic of  $[100]$ -oriented FCC Au nanowire used in this work. The nanowire has a diameter of 1.5 nm and length 12.3 nm, where the last two rows on atoms on the left and right hand sides, colored green and red, respectively, are held fixed.

The Au-Au interactions are described by using the TB-SMA potential [16]. The low computational cost of TB-SMA enables us to carry out a statistically meaningful number of simulations. Moreover, TB-SMA has been shown to reproduce the energetic and structural characteristics of elongating Au nanowires better than other popular semi-empirical potentials, when compared with density functional theory calculations [5]. The simulations are carried out with the LAMMPS molecular dynamics package [17], extended to include the TB-SMA potential. The equations of motion are integrated by using the velocity Verlet algorithm with a time step of 2.0 fs. The temperature of the nanowires is controlled by using a Nosé-Hoover thermostat.

### 2.2. Order parameters

Inherent to most order parameter schemes is an implicit concept of matching; order parameters typically quantify how closely a given structure matches an ideal or reference state. This concept has been generalized in the computer science field of “shape matching” [13], which has recently been applied to a wide class of particle-based systems, including model nanomaterials [14, 15]. The shape matching scheme can be broken down into two main components: *shape descriptors* and *matching metrics*. Shape descriptors are numerical representations of the underlying structural pattern(s) of the system, constructed such that they can be represented as scalars/vectors of real and/or imaginary components. In this work, we use a spherical harmonics shape descriptor, as it is well suited to the types of structural changes visually identified in previous studies of mechanically deformed nanowires (see [14, 18] for more details

on spherical harmonics). Since shape descriptors are represented as vectors, the degree to which two identically constructed shape descriptors match can be assessed by using simple vector operations; here we use the normalized dot product as the matching metric. A basic order parameter is therefore constructed by calculating the dot product between a reference shape descriptor and the shape descriptors calculated from the atoms within the nanowire.

In all cases, we only consider the first neighbor shell of each atom and use this as input to the spherical harmonics shape descriptor. Reference shape descriptors are defined in an identical manner, i.e., they contain only first neighbor information. Because of the flexibility of this approach, new order parameters can be trivially constructed by changing the reference structure; for example, a simple FCC order parameter can be constructed by using an ideal FCC state as reference, or a self-similarity correlation function can be constructed by using the initial structure of the nanowire as the reference [14,15]. One needs only to understand this general framework, in order to understand how each *ad hoc* order parameter is constructed; we discuss the specifics of each order parameter below.

### 3. Results

The rate-dependent energy release mechanism states that low-energy modes of relaxation, such as crystal dislocations, are more likely to occur for wires elongated at high temperature or at a low rate of elongation. Visually, we observe that for systems exhibiting low energy modes, structural rearrangements tend to occur throughout the entire wire, while for high-energy modes, structural rearrangements tend to be localized to a single region (i.e., the neck), leaving most of the wire in its original state. This can be visually observed in Figs. 2a,b for example wires at  $T=0.01\text{K}$  (high energy modes) and  $T=298\text{K}$  (low energy modes), respectively.

We devise a self-similarity order parameter ( $OP_{ss}$ ) to quantify this behavior, where  $OP_{ss} = 1$  corresponds to an ideal match with no change in either structure or orientation. As a function of elongation, we compare each atom with its original, unstretched state at  $\Delta X = 0$ . Here we use the spherical harmonics *vector* that is sensitive to both structure and orientation, with  $\ell = 6$  [14, 18]. Note that for low energy modes, such as reorientation of the crystal lattice, one must use a shape descriptor that is sensitive to orientation to detect this change. Figure 2c plots the average value of  $OP_{ss}$  just prior to the nanowire breaking, as a function of rate of elongation for wires stretched at temperatures  $T=0.01\text{K}$  and  $T=298\text{K}$ . Each datapoint represents the average of 50 independent simulations. For systems at  $T=0.01\text{K}$ , there appears to be crossover in behavior at  $\sim 0.5$  m/s. Wires pulled at rates  $> 0.5$  m/s demonstrate a rapid increase in  $OP_{ss}$  with increasing rate of elongation; thus, the frequency of observing low-energy relaxations decreases as the rate increases. Wires pulled at  $< 0.5$  m/s do not demonstrate a strong rate dependence but do have a lower value of  $OP_{ss}$  than do systems in the higher rate regime. While this behavior is not discernible from visual inspection, the calculation of  $OP_{ss}$  allows us to observe this trend. Wires at  $T=298\text{K}$  demonstrate a steady increase in  $OP_{ss}$  as the rate of elongation is increased, which can be interpreted as a decrease in the number of low-energy relaxation modes. We note that the average  $OP_{ss}$  for nanowires at  $T=298\text{K}$  is lower than those at  $T=0.01\text{K}$  for all elongation rates; this result supports the previous assertion by the rate-dependent energy release mechanism that low energy modes of relaxation are more likely for high temperature states.

For a more detailed examination, we explore the onset of necking for the wires. As a typical nanowire elongates, a small region begins to neck, becoming narrower than the original diameter of the wire. The neck forms in order to enable the bulk of wire to relax its configuration, localizing the higher energy structural modes to a single location. Even if a wire undergoes a large number of low energy relaxations, a neck will still form prior to breaking. Structurally, we observe that atoms within the neck are strongly perturbed from their original structure, often demonstrating noncrystalline local structures. Thus, we can quantify neck formation by using a similar order parameter to the previously defined  $OP_{ss}$ . As before, we compare the structure

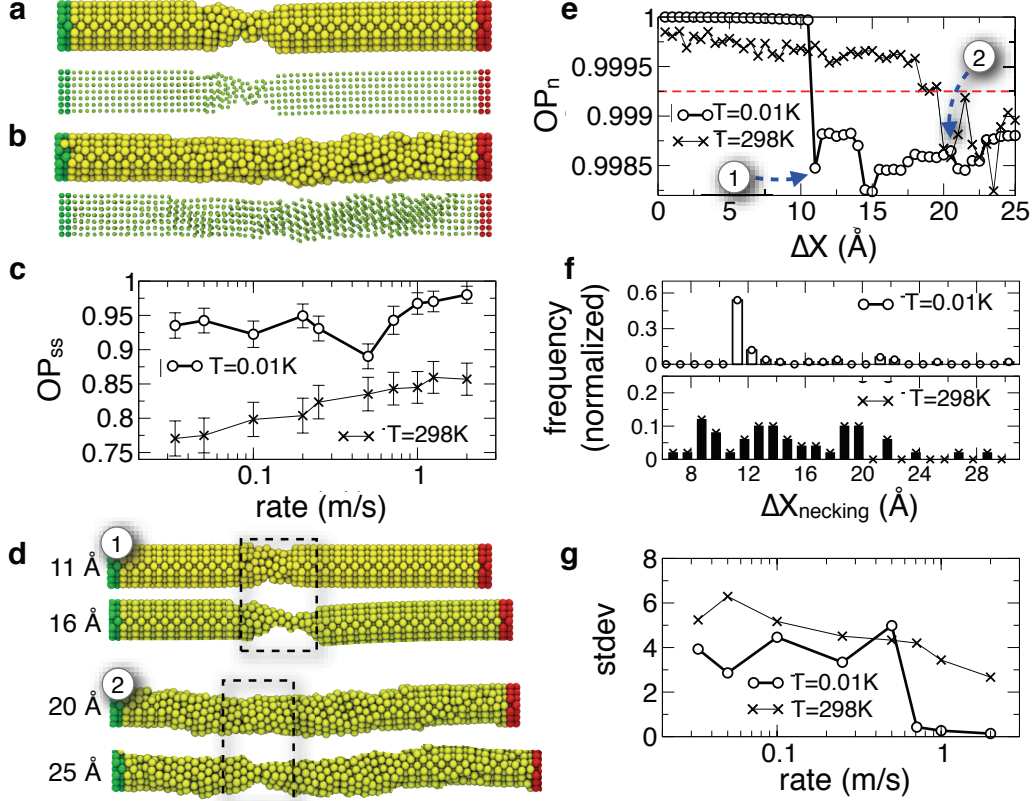


**Figure 2.** (a) Simulation snapshot of a prototypical wire elongated at 0.1 m/s and  $T=0.01\text{K}$ . The lower image is identical but with atoms shown at 25% of their true diameter for clarity. (b) Identical to (a), but at  $T=298\text{K}$ . (c)  $OP_{ss}$  as a function of rate for  $T = 0.01\text{K}$  and  $T=298\text{K}$ . (d) Two example wires at  $T=0.01\text{K}$  (1) and  $T=298\text{K}$  (2) shown at the onset of necking and 5 Å after necking occurs; both wires are elongated at 0.1 m/s. The neck regions are highlighted in both wires. (e)  $OP_n$  of the two wires shown in (d), where labels (1) and (2) indicate the onset of necking for each wire, determined visually. (f) Histograms of the onset of necking for  $T=0.01\text{K}$  and  $T=298\text{K}$  for systems elongated at 0.1 m/s; both histograms are generated from 50 independent simulations. (g) Standard deviation of the onset of necking plotted as a function of rate for  $T=0.01\text{K}$  and  $T=298\text{K}$ .

of the wire with its original state at  $\Delta X = 0$  but now use a rotationally invariant description of the atoms, calculated by taking the *magnitude* of the spherical harmonics vector [14, 18]; that is, our shape descriptor is sensitive only to structure, not orientation of that structure. Ignoring orientational changes will avoid misidentifying low energy modes, such as crystal reorientation, as neck formation. Since only a small number of particles are typically involved in the neck formation, a systemwide average is not likely to be sensitive enough; as proposed in Ref. [15], we can instead use the standard deviation of the match ( $M_{<stdev>}$ ) to detect when this subset of atoms deviates strongly from their original state. For consistency, we define our order parameter of necking as  $OP_n = 1 - M_{<stdev>}$ , such that perfect ordering coincides with  $OP_n = 1$ .

Figures 2d,e show the representative behavior of prototypical wires at  $T=0.01\text{K}$  and  $T=298\text{K}$ , elongated at 0.1 m/s. In Fig. 2d, we visually observe that the  $T=0.01\text{K}$  wire forms a neck at  $\Delta X = 11\text{ Å}$ , which correlates to the rapid drop in the value of  $OP_n$  (labeled as (1) in Fig. 2e). The wire at  $T=298\text{K}$  is visually determined to have an onset of necking at  $\sim 20\text{ Å}$  in

fig. 2d, which also correlates to a rapid drop in order parameter (labeled as (2) in Fig. 2e). To aggregate this data, we define the onset of necking as  $OP_n < 0.99925$ , which satisfies the behavior at both temperatures. Figure 2f plots histograms of the onset of necking constructed from 50 simulations at  $T=0.01\text{K}$  and 50 simulations at  $T=298\text{K}$  for wires elongated at  $0.1\text{ m/s}$ , calculated by using the previously determined criteria. For wires elongated at  $T=0.01\text{K}$ , the onset of neck formation is rather uniform, where  $\sim 65\%$  of the systems neck at  $11\text{--}12\text{ \AA}$ . The additional  $\sim 35\%$  of systems neck at larger elongations as a result of forming lower energy crystal reorientations prior to neck formation, observed visually. Conversely, wires elongated at  $T=298\text{K}$  demonstrate a broad distribution of necking, which can be attributed to the predominance of low energy relaxation modes at higher temperature. Thus, a second convenient metric for quantifying low energy relaxation modes, at least for the early stages of elongation, is to examine the standard deviation of the distribution of the onset of necking, where larger values indicate the formation of more low energy relaxation modes. Figure 2g plots the standard deviation of necking as a function of rate. We see similar trends to Fig. 2b, where there is a clear crossover at  $0.5\text{ m/s}$  for  $T=0.01\text{K}$ , and a gradual change for  $T=298\text{K}$ .

#### 4. Conclusion

We have demonstrated the use of order parameters to detect structural changes within elongated Au nanowires, developed within the general shape-matching framework [13–15]. These order parameters allow us to directly quantify behavior that was previously observed only visually. Our analysis lends strong support to the rate-dependent energy release mechanism proposed by our group in [6]. This general approach to structural analysis may prove valuable insight regarding the correlation between structure and the transport properties of elongated nanowires, as well as to elucidate the structural changes that occur when nanowires are “cold welded,” as shown in recent experiments [19].

#### References

- [1] Scheer E, Agrait N, Cuevas J C, Yeyati A L, Ludoph B, Martin-Rodero A, Bollinger G R, van Ruitenbeek J M and Urbina C 1998 *Nature* **394** 154–157
- [2] Yanson A I, Bollinger G R, van den Brom H E, Agrait N and van Ruitenbeek J M 1998 *Nature* **395** 783–785
- [3] Rodrigues V and Ugarte D 2001 *Phys. Rev. B* **63** 1–4
- [4] Coura P Z, Legoas S B, Moreira A S, Sato F, Rodrigues V, Dantas S O, Ugarte D and Galvao D S 2004 *Nano Lett.* **4** 1187–1191
- [5] Pu Q, Leng Y, Tsetseris L, Park H S, Pantelides S T and Cummings P T 2007 *J. Chem. Phys.* **126** 1–6
- [6] Pu Q, Leng Y and Cummings P T 2008 *J. Am. Chem. Soc.* **130** 17907–17912
- [7] Wang D, Zhao J, Hu S, Yin X, Liang S, Liu Y and Deng S 2007 *Nano Lett.* **7** 1208–1212
- [8] Tavazza F, Levine L E and Chaka A M 1009 *J. Appl. Phys.* **106**
- [9] Hakkinen H, Barnett R N, Scherbakov A G and Landman U 2000 *J. Phys. Chem. B* **104** 9063–9066
- [10] Ono T and Hirose K 2005 *Phys. Rev. Lett.* **94** 1–4
- [11] Jelinek P, Perez R, Ortega J and Flores F 2008 *Phys. Rev. B* **77** 1–12
- [12] Tavazza F, Levine L E and Chaka A M 2010 *Phys. Rev. B* **81** 1–12
- [13] Veltkamp R C and Hagedoorn M 2001 *Principles of visual information retrieval* 87
- [14] Keys A S, Iacovella C R and Glotzer S C 2011 *Annual Review of Condensed Matter Physics* **2** 263–285
- [15] Keys A S, Iacovella C R and Glotzer S C 2011 *J. Comput. Phys.* doi:10.1016/j.jcp.2011.04.017
- [16] Cleri F and Rosato V 1993 *Phys. Rev. B* **48** 22–33
- [17] Plimpton S 1995 *J. Comput. Phys.* **117** 1–19
- [18] Steinhardt P J, Nelson D R and Ronchetti M 1983 *Phys. Rev. B* **28** 784–805
- [19] Lu Y, Huang J Y, Wang C, Sun S and Lou J 2010 *Nature Nanotech.* **5** 218–224